REPORT DOCUMENTATION PAGE

1. REPORT DATE (DD-MM-YYYY) 11 June 2003	2. REPORT TYPE Technical Paper	3. DATES COVERED (From - To)

4. TITLE AND SUBTITLE

An Automated Fluid-Structural Interaction Analysis of a Large Segmented Solid Rocket Motor

5a. CONTRACT NUMBER
F04611-99-C-0002

5b. GRANT NUMBER

5c. PROGRAM ELEMENT NUMBER

6. AUTHOR(S)

Brian Rex, Qunzhen Wang, Darson Isaac

5d. PROJECT NUMBER
1011

5e. TASK NUMBER
00TN

5f. WORK UNIT NUMBER

7. PERFORMING ORGANIZATION NAME(S) AND ADDRESS(ES)

ATK Thiokol
9160 N. Highway
P.O. Box 707
Brigham City, UT 84302-0707

8. PERFORMING ORGANIZATION REPORT NUMBER

AFRL-PR-ED-TP-2003-156

9. SPONSORING / MONITORING AGENCY NAME(S) AND ADDRESS(ES)

Air Force Research Laboratory (AFMC)
AFRL/PRS
5 Pollux Drive
Edwards AFB CA 93524-7048

10. SPONSOR/MONITOR'S ACRONYM(S)

11. SPONSOR/MONITOR'S NUMBER(S)

AFRL-PR-ED-TP-2003-156

12. DISTRIBUTION / AVAILABILITY STATEMENT

Approved for public release; distribution unlimited.

13. SUPPLEMENTARY NOTES

14. ABSTRACT

20030801 116

15. SUBJECT TERMS

16. SECURITY CLASSIFICATION OF:			17. LIMITATION OF ABSTRACT	18. NUMBER OF PAGES	19a. NAME OF RESPONSIBLE PERSON Sheila Benner
a. REPORT Unclassified	b. ABSTRACT Unclassified	c. THIS PAGE Unclassified	A		19b. TELEPHONE NUMBER (include area code) (661) 275-5693

MEMORANDUM FOR PRS (Contractor Publication)

FROM: PROI (STINFO)   11 Jun 2003

SUBJECT: Authorization for Release of Technical Information, Control Number: **AFRL-PR-ED-AB-2003-156**
Brian Rex, Qunzhen Wang, and Daron Isaac (ATK Thiokol), "An Automated Fluid-Structural
Interaction Analysis of a Large Segmented Solid Rocket Motor"

AIAA Joint Propulsion Conference   (Statement A)
(Huntsville, AL, 20-23 July 2003) (Deadline: None Listed)

AIAA-2003-4507
An Automated Fluid-Structural Interaction Analysis of a Large Segmented Solid Rocket Motor

Brian W. Rex , Qunzhen Wang, and Daron Isaac
ATK Thiokol Propulsion Corp.
Brigham City, UT

39th AIAA/ASME/SAE/ASEE Joint Propulsion Conference and Exhibit
July 20-23, 2003
Huntsville, AL

An Automated Fluid-Structural Interaction Analysis of a Large Segmented Solid Rocket Motor

Brian W. Rex , Qunzhen Wang, and Daron Isaac
Science and Engineering
ATK Thiokol Propulsion Corp., Brigham City, UT 84302

The ETM-3 motor is basically an RSRM motor with an additional center segment added. The propellant burn rate was lowered to account for the additional surface area of the motor and the nozzle throat diameter was increased. The additional segment also increased mass flow and mach number in the motor. Because of this harsher flow environment, it was thought necessary to chamfer the leading edges of every segment and conduct a detailed fluid/structural interaction (FSI) analysis to ensure propellant grain stability against boot-strapping. The analyses showed that the addition of the 3 inch radial by 24 inch axial chamfer on the leading edges of the center/forward, center, center/aft, and aft segments was sufficient to give the ETM-3 motor stable grain displacements at much lower than expected propellant moduli. This report documents the FSI analysis work done for ETM-3.

The analyses conducted and documented in this report assumed linear elastic material behavior and quasi-steady state fluid behavior without time response in either the structural or fluid models. Thus, the analyses represented only an approximation at a single snapshot in time. This led to selecting the largest chamfer size analyzed herein to get the biggest safety factor against boot-strapping.

INTRODUCTION

The ETM-3 motor is basically an RSRM motor with an additional center segment added to the original 4 segments. The propellant burn rate was lowered to account for the additional surface area of motor. The additional segment also increased mass flow and mach number in the motor, even with the lower burn rate. Because of this harsher flow environment, it was necessary to conduct a detailed fluid/structural interaction (FSI) analysis to ensure propellant grain stability against boot strapping.

Boot-strapping is the name given to the phenomenon where flow in the rocket motor imposes pressure on the propellant grain, which displaces in response, which then leads to flow changes, which produce even more grain displacement until flow is ultimately blocked or the grain fails.

TEST ARTICLE DESCRIPTION

The ETM-3 motor was a 5 segment RSRM type motor. The RSRM has 4 segments. Thus, one segment was added to create the ETM-3 motor. The propellant used in the motor was TP-H1148, Type VII, which is basically RSRM propellant with different AP grind ratios and different burn rate catalyst. The ETM-3 motor was to be static tested in summer of 2003, at T-97, Promontory, Utah. The center and aft segments of ETM-3 had 3 inch radial and 24 inch axial chamfers on the forward bore surfaces.

METHOD OF ANALYSIS

Boot strapping in a solid rocket motor is both an undesirable and complex phenomenon involving interaction between the flow/ballistics and grain structure of the motor itself. The analysis method used in this report used an automated, iterative procedure between a steady-state CFD flow solution and a linear elastic deformation

analysis. FLUENT® software was used for the flow solution, while ABAQUS® was used for the structures solver. The procedure was automated between the two solvers with FEM Builder®, an in-house, finite element, pre- and post-processor, and Python scripting language.

The procedure was as follows:

1. Fluid and solid models are prepared and linked with FEM Builder®/Python Script
2. FEM Builder®/Python script is started, which calls FLUENT®
3. FLUENT®calculates flow (pressures) on nominal geometry
4. Pressures from FLUENT® solution are applied to structural model (nominal geometry) automatically with FEM Builder®/Python script
5. ABAQUS® calculates deformations for the applied pressure
6. These deformations (or some percentage of them) are applied to

the fluid grid, which is then re-meshed and smoothed.
7. FLUENT® calculates flow (pressure) for the second time
8. Pressures from FLUENT® solution are applied to structural model (nominal geometry) automatically with FEM Builder®/Python script
9. Process continues until maximum number of iterations specified or until convergence of the solid model is reached (grain is no longer moving between each iteration)
10. Each Fluid-Structural Interaction (FSI) analysis is performed with a fixed propellant modulus
11. Critical modulus is determined to be the value at which the grain deformations are stable (i.e. not changing with iteration)

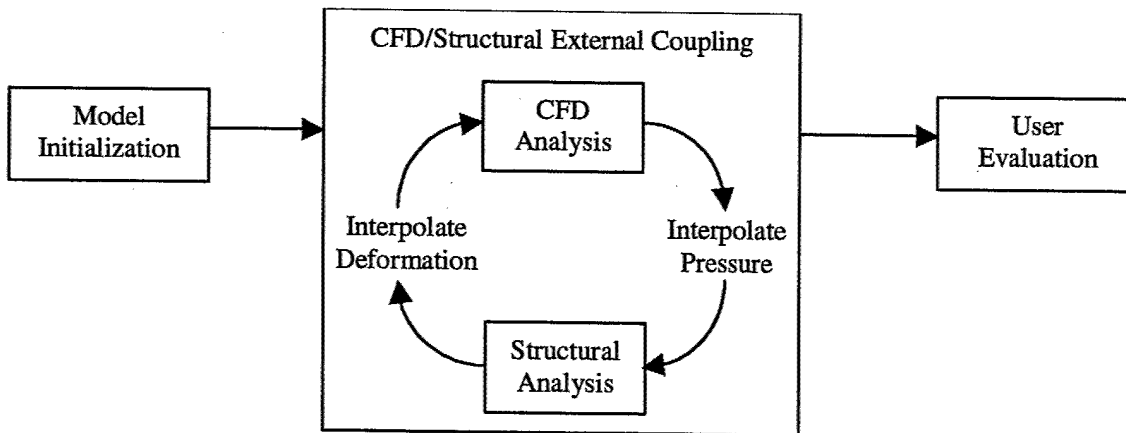A schematic of the foregoing FSI analysis process description is shown in Figure 1.


Figure 1. Schematic of FSI Analysis Process

STRUCTURAL MODELS

Portions of the structural models of ETM-3, with and without various sizes of chamfers are shown in Figures 2 through 5. All segments of ETM-3 were modeled, even though only a portion is shown in the figures. Figure 6 shows the outline of the entire motor, and the location of the critical slot for boot strapping.

2
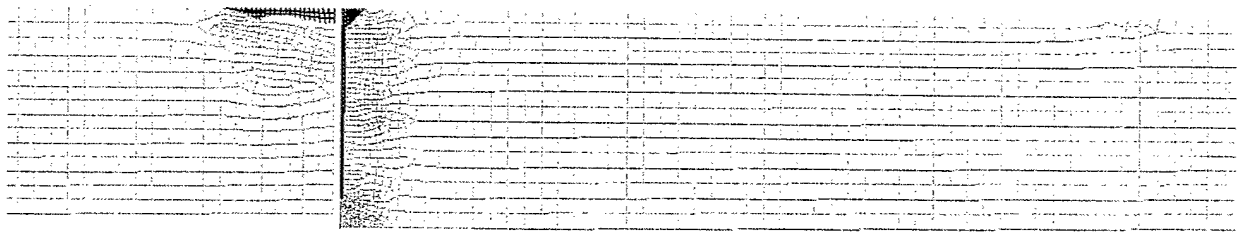
Figure 2. Structural Model of ETM-3, Nominal Geometry, No Chamfers
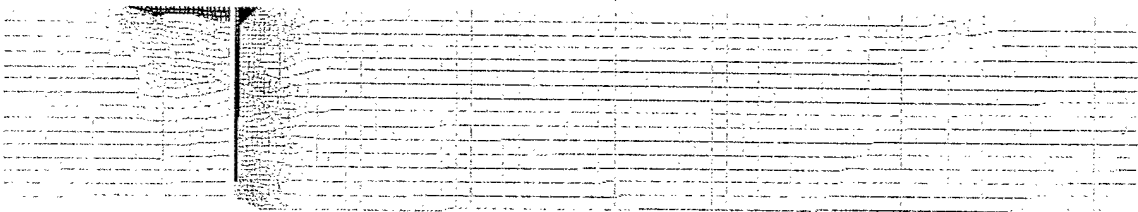
Figure 3. Structural Model of ETM-3, Nominal Geometry, 3 x 6 inch Chamfers
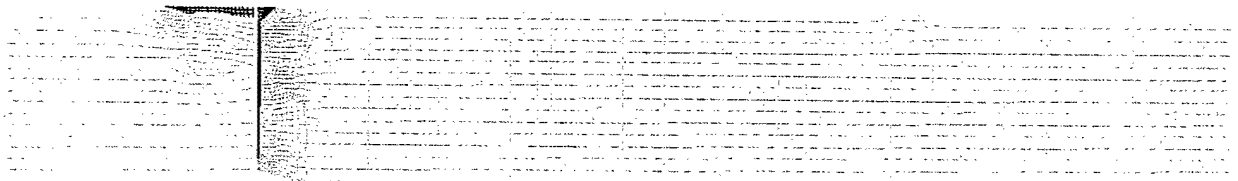
Figure 4. Structural Model of ETM-3, Nominal Geometry, 3 x 12 inch Chamfers

Figure 5. Structural Model of ETM-3, Nominal Geometry, 3 x 24 inch Chamfers

Forward

Aft

Critical Slot for boot strapping

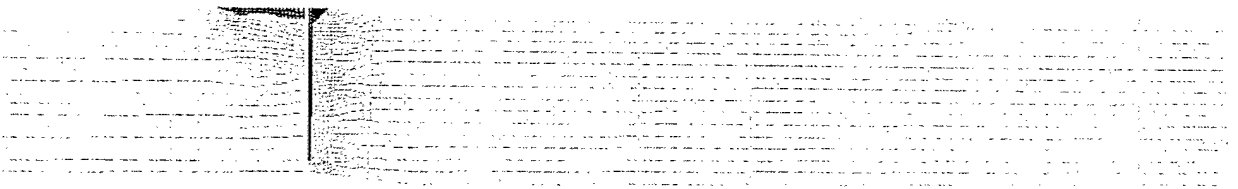**Figure 6. Structural Model of ETM-3 showing critical slot for boot strapping**

BOUNDARY CONDITIONS FOR STRUCTURAL/FLUID MODELS

A summary of the boundary conditions analyzed in this report is shown in Table 1. The fluid models used the burn rates shown to compute pressures that were applied to the structural models as boundary conditions. Additional boundary conditions used in the structural models are also shown. The head end pressures calculated for the given burn rates are shown in the table for reference. No horizontal slump loading was included with any of the models because of the 2-D limitations of the models.

The last three analyses shown in Table 1 were performed to provide converged pressure boundary conditions for the PLI structural analyses. Furthermore, these analyses were performed at the expected propellant moduli based on Reference 1, namely 990 and 2150 psi for 90° and 40°F, respectively. The analysis at 55°F was performed at 1675 psi propellant modulus, which was determined by interpolation of the 50°F and 60°F data from TR-12874.

Table 1. Summary of Boundary Conditions

Motor	Configuration	2-D Burn Rate for Pressure Boundary Conditions	Head End Pressure (for Ref.)	Temp Load	Slump	Propellant Modulus
ETM-3	no chamfer, nominal geometry	**MEOP** .343 in/sec propellant 1.629 in/sec fin propellant	~940 psi	SFT to 70°F	no	varying to determine critical modulus
ETM-3	3 x 6 chamfer, nominal geometry	**MEOP** .3698 in/sec propellant 1.7563 in/sec fin propellant	~1023 psi	SFT to 70°F	no	varying to determine critical modulus
ETM-3	3 x 12 chamfer, nominal geometry	**MEOP** .361 in/sec propellant 1.7147 in/sec fin propellant	~1010 psi	SFT to 70°F	no	varying to determine critical modulus
ETM-3	3 x 24 chamfer, nominal geometry	**MEOP** .361 in/sec propellant 1.7147 in/sec fin propellant	~1010 psi	SFT to 70°, 80°, or 90°F	no	varying to determine critical modulus
Converged Analyses Used for PLI Structural Analysis Boundary Conditions						
ETM-3	3 x 24 chamfer, nominal geometry	**MEOP** .3635 in/sec propellant 1.7261 in/sec fin propellant	1011 psi	SFT to 90°F	no	990 psi
ETM-3	3 x 24 chamfer, nominal geometry	**MEOP** .3381 in/sec propellant 1.6057 in/sec fin propellant	913 psi	SFT to 40°F	no	2150 psi
ETM-3	3 x 24 chamfer, nominal geometry	**MEOP** .3492 in/sec propellant 1.6581 in/sec fin propellant	955 psi	SFT to 55°F	no	1675 psi

FLUID MODELS

In the fluid-structural analysis shown in this report, FLUENT® version 5.6 is used as the flow solver. FLUENT® is a state-of-the-art CFD code written in the C programming language for modeling fluid flow and heat transfer problems. FLUENT® has been used in a number of internal motor flow analyses. See Reference 2. The flow is assumed to be steady-state and 2D axisymmetric. The 3D fin regions near the headend of ETM-3 are taken into account by adjusting the burn rate coefficient such that the total propellant

surface area is modeled correctly. It was also assumed that the combustion gas is a single-phase, chemically frozen, calorically perfect gas. That is, the fluid is assumed to be a homogeneous mixture of gas and particles with an equivalent molecular weight while no combustion model is applied and no real gas effect is taken into account.

Both pressure-based and density-based solvers are available in FLUENT® although only the former is used in this work. While various turbulence models and near-wall treatments are implemented in FLUENT®, the two-equation RNG k-ε model with the standard wall function is applied. The constants in the RNG k-ε model used are C_μ=0.06, $C_{\varepsilon 1}$=1.42, and $C_{\varepsilon 2}$=1.68 while the wall Prandtl number is 0.85. The turbulence viscosity ratio is limited to 10,000.

The propellant surface is modeled in FLUENT® by a mass inflow boundary condition with the mass flow rate being calculated as

$$\dot{m} = ap^n \rho_s A$$

where p is the static pressure, ρ_s is the density of the propellant and A is the surface area. The burn rate coefficient a and the exponential n depend on the formulation of the propellant. In this work, a burn rate exponential of 0.35 is used for RSRM whereas 0.32 is used for ETM-3. At the propellant boundaries, a turbulence intensity of 5% and a turbulent viscosity ratio of 100 are applied. A flame temperature of 3387 K is also specified. The inhibitor and nozzle walls are modeled by the adiabatic wall boundary condition while the nozzle exit plane is modeled as the pressure outlet boundary condition.

Figures 7 - 10 show the pressure and Mach number contours predicted from FLUENT® before coupling with ABAQUS® for both RSRM and ETM-3. The computational domain for the fluid is the whole motor including headend, slots and nozzle.
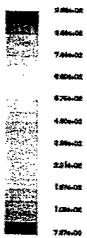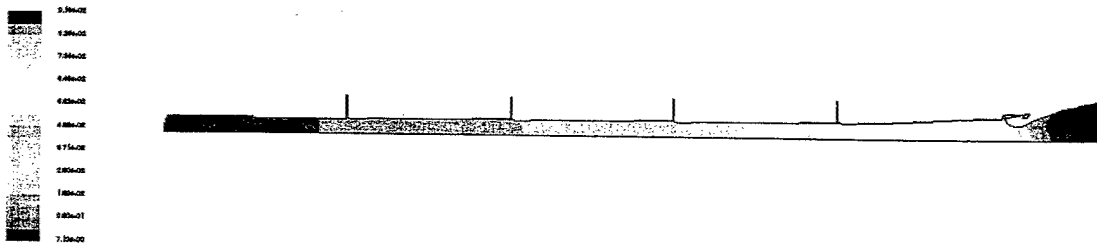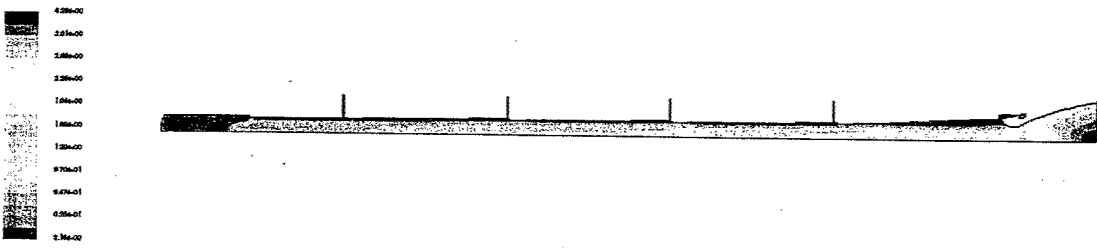

Figure 7: Pressure in RSRM.
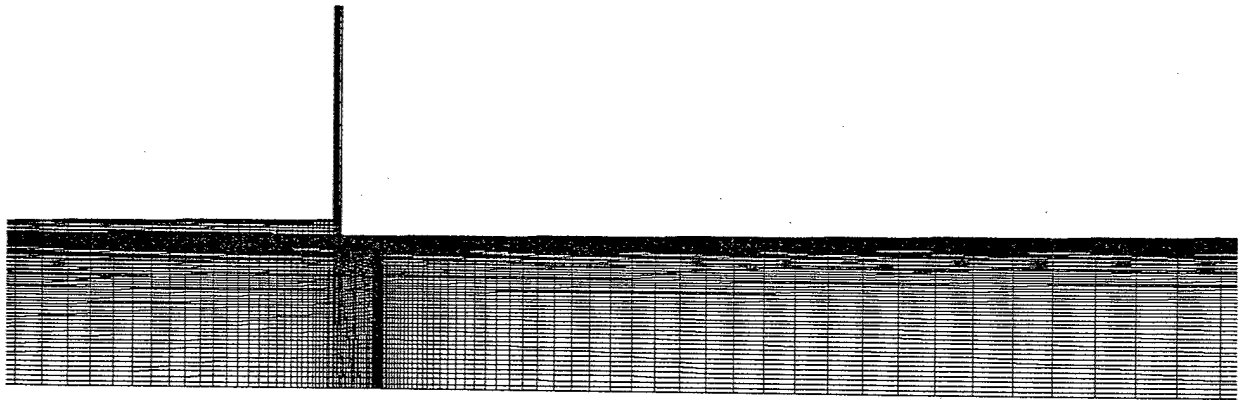

Figure 8: Mach number for RSRM.
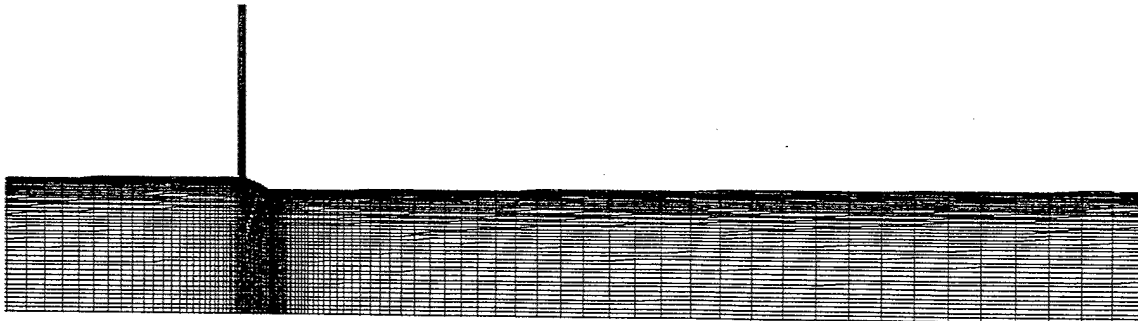
Figure 9: Pressure for ETM-3.

Figure 10: Mach number for ETM-3.

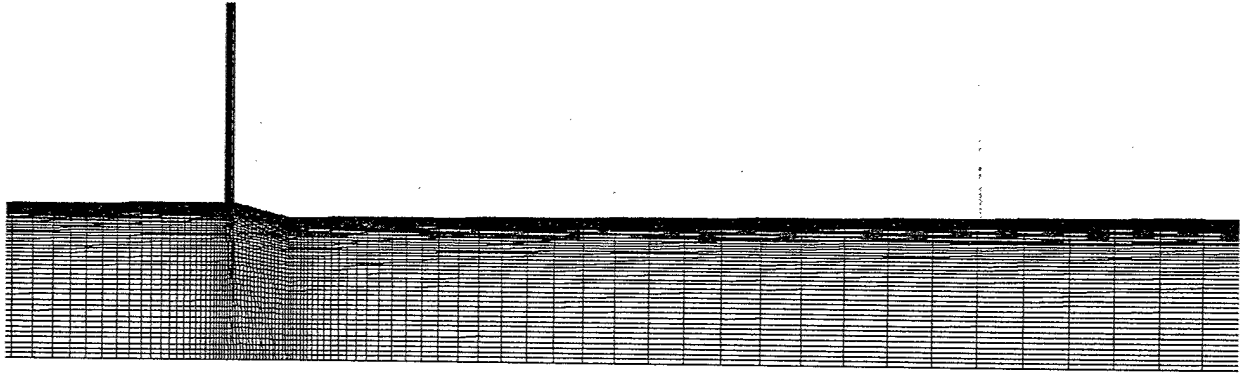A close-up of the fluid models (portions) of ETM-3, with and without chamfers are shown in Figures 11 through 14. As mentioned before, all segments of both motors were modeled, including the nozzles, even though only a portion is shown here.
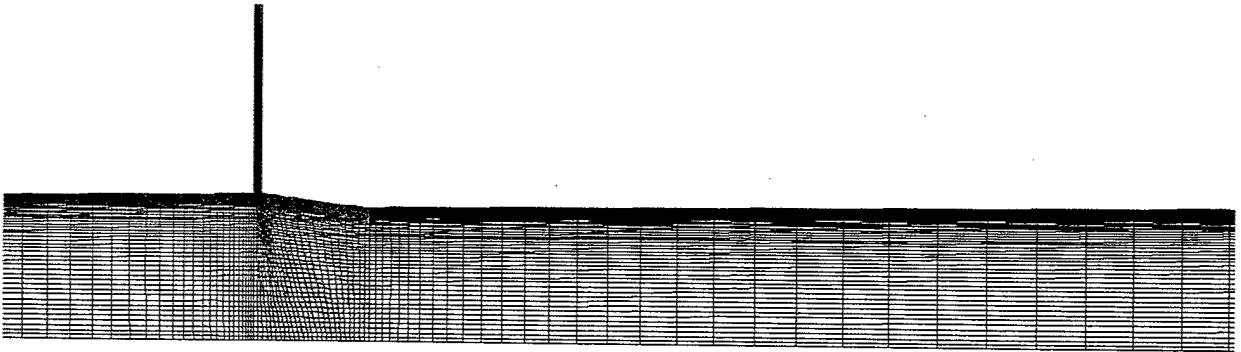

Figure 11. Fluid Model of ETM-3, No Chamfers

Figure 12. Fluid Model of ETM-3, 3 x 6 Chamfers

Figure 13. Fluid Model of ETM-3, 3 x 12 Chamfers

Figure 14. Fluid Model of ETM-3, 3 x 24 Chamfers

MECHANICAL PROPERTIES ASSESSMENT

The FSI analyses of ETM-3 presented in the proceeding sections assumed that the propellant mechanical properties of TP-H1148 Type IV and TP-H1148 Type VII were identical. This assumption regarding the relaxation modulus was confirmed by the mechanical properties report for TP-H1148 Type VII, as documented in Reference 3.

Further study of the ignition modulus properties, shown in Table 2, of TP-H1148 Type IV were documented in Reference 1. This work was based on a number of studies, whose details were not covered here. Only the ignition modulus values from that report are presented in this document.

Additionally, high rate, bi-rate-and-hold testing on TP-H1148 was performed to verify the moduli and is documented in Reference 4. This testing confirmed that the ignition modulus values used were conservative.

Table 2. Ignition Modulus Values from TR12874 (in psi)

T	Modulus
°F	.6 sec
40	2150
50	1800
60	1550
70	1300
75	1200
80	1100
90	990

RESULTS OF ANALYSES

The resulting deformations of the propellant grain from each iteration between the fluid and structural models were scrutinized. From these observations, it was obvious that a particular slot (joint between segments) was of interest. (See Figure 6.) This is where the potential for boot-strapping existed. A few iterations at the critical slot for ETM-3 without chamfers are shown in Figure 15. These iterations showed that the slot widened and the leading edge corner of the grain moved radially inward.
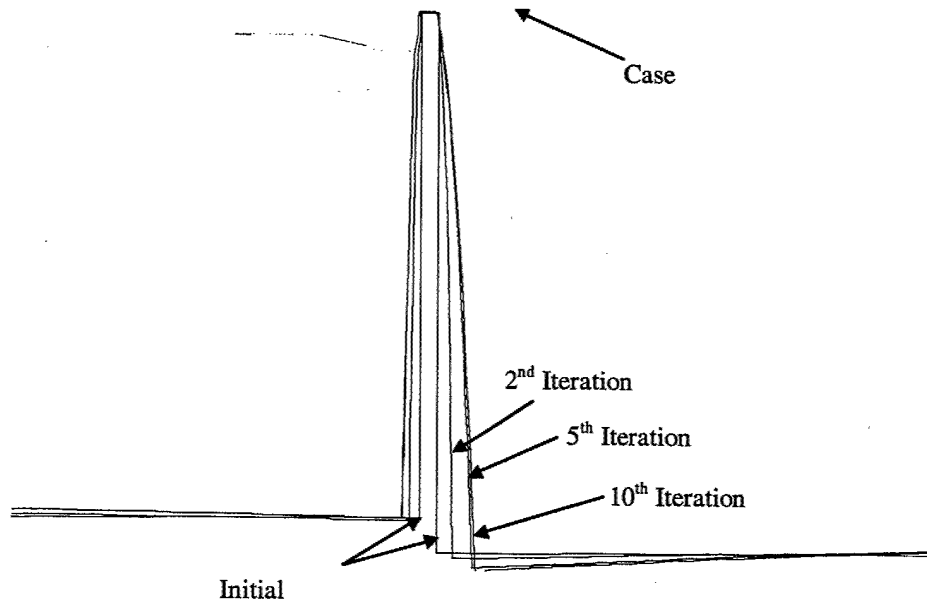
Figure 15. Sample Deformation Results at Critical Slot for ETM-3 Without Chamfers

Numerous FSI analyses were conducted in the above manner while varying the propellant modulus of the structural model. Of course, the deformations at the critical slot (and all other locations) were effected by the changing stiffness of the propellant. These many results were condensed into Figure 16 by only plotting the radial grain deformations at the critical slot of ETM-3, with and without chamfers, versus modulus.
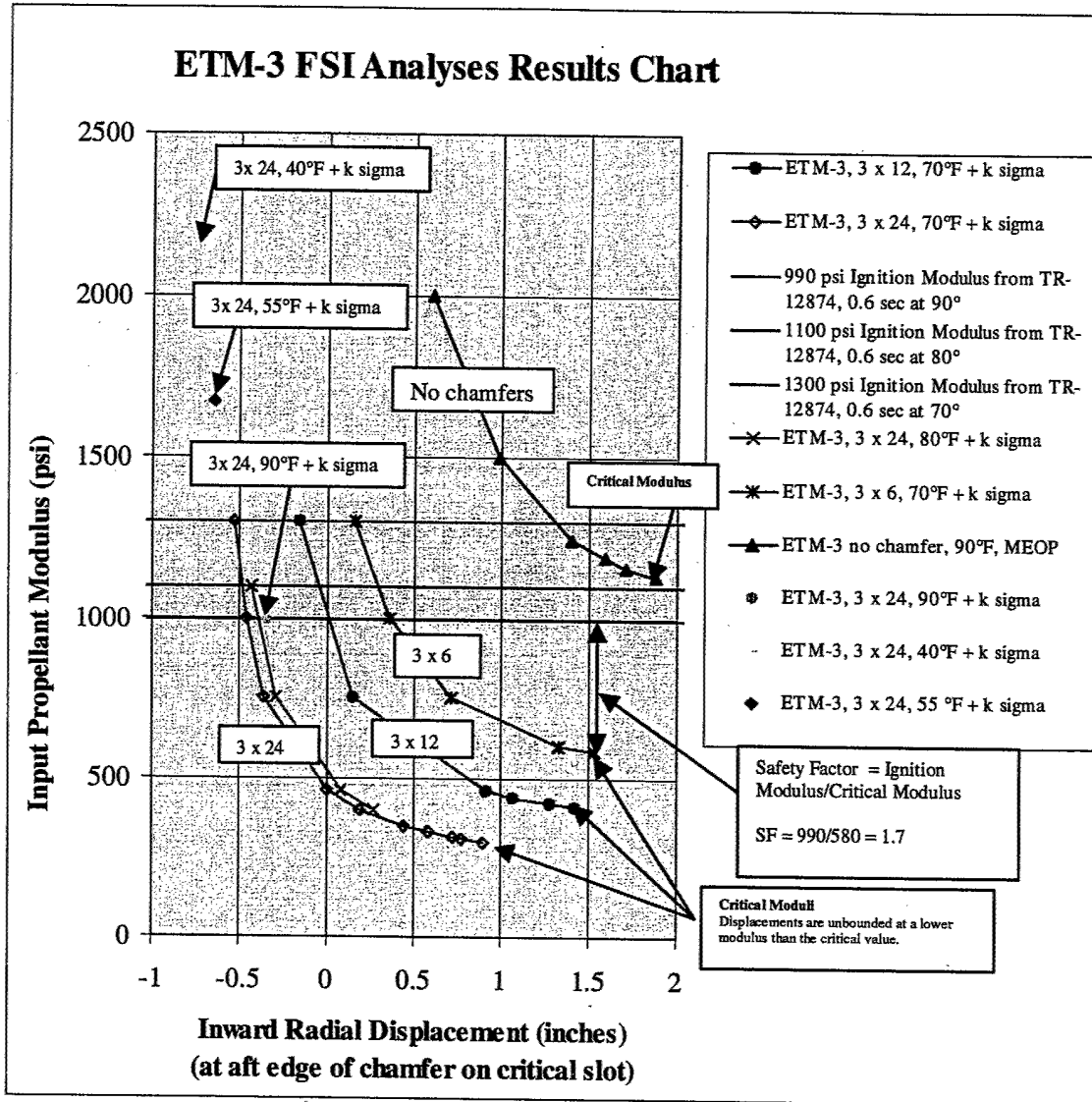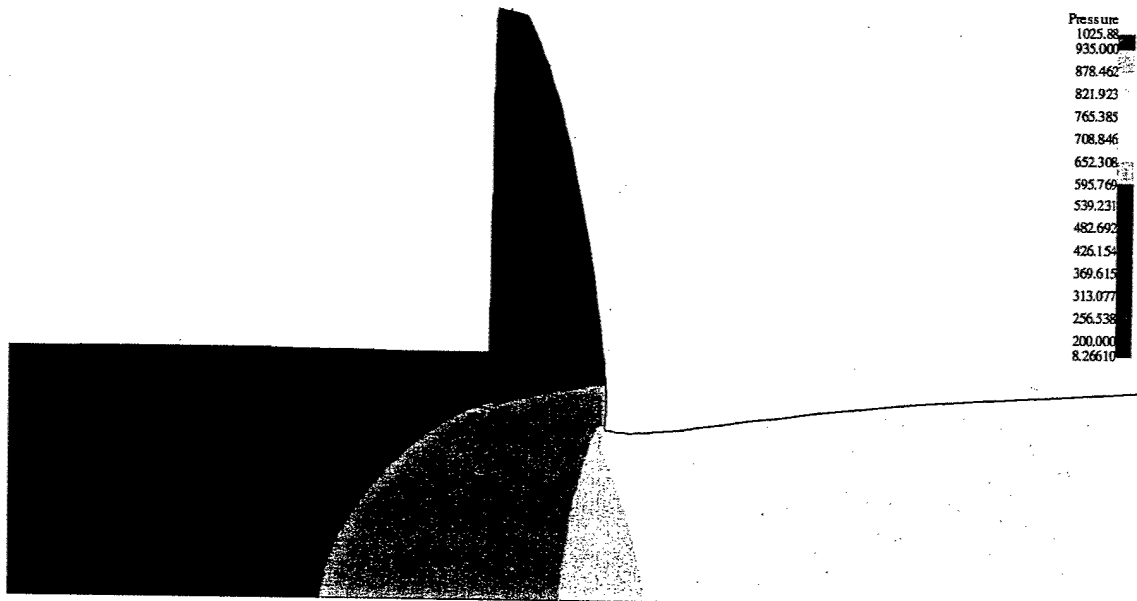
9

Figure 16. ETM-3 FSI Analyses Results

The critical modulus for each motor/burn rate condition was the propellant modulus at which the propellant grain at the critical slot would reach a stable position through multiple fluid/structural iterations at that modulus. Figure 16 shows that when a FSI analysis was run at a propellant modulus less than the critical value, the grain displacements would be unstable, meaning they would continue to increase and cause flow restriction and eventual bore choking in the motor. The effect on flow of this unbounded grain displacement is shown in Figure 17.

Pressure
1025.88
935.000
878.462
821.923
765.385
708.846
652.308
595.769
539.231
482.692
426.154
369.615
313.077
256.538
200.000
8.26610

Figure 17. Flow Restriction Due to Low Propellant Modulus

The critical moduli were then used to calculate safety factors using the following formula.

$$SafetyFactor = \frac{IgnitionModulus}{CriticalModulus}$$

The safety factors for the 3 sizes of chamfers at 3 temperatures are summarized in Table 3.

Table 3. Safety Factors Against Boot Strapping

Chamfer Size (inches)	Temperature (°F)	Ignition Modulus (TR-12874, psi)	Critical Modulus (psi)	Safety Factor (Ignition modulus/Critical modulus)
3 x 6	70	1300	570	2.3
	80	1100	580	1.9
	90	990	590	1.7
3 x 12	70	1300	410	3.2
	80	1100	420	2.6
	90	990	430	2.3
3 x 24	70	1300	300	4.3
(expected static test temperature)	80	1100	310	3.6
	90	990	320	3.1

(Note: The critical moduli for some of the conditions were extrapolated based on the well behaved family of curves for the 3 x 24 chamfer at 70, 80, and 90°F.)

DISCUSSION

The lowest safety factor against bore choking was 1.7 for a 3 x 6 chamfer at 90°F. The safety factor increased to 3.1 for a 3 x 24 chamfer at 90°F, which further increased to a 3.6 safety factor at 80°F. This represented the approximate expected static test temperature for ETM-3.

The family of curves for each chamfer size of varying modulus and radial displacement was well behaved and showed increasing safety factor with increasing chamfer size. This gave confidence that the analyses were providing consistent results, though not necessarily absolutely correct.

CONCLUSIONS

It was concluded that 3 x 24 inch chamfers would be desirable because they gave the largest safety factors against boot-strapping. Also, without chamfers, ETM-3 would experience boot-strapping.

The critical propellant modulus for ETM-3, with 3 by 24 inch forward bore chamfers, at MEOP and 80°F was 310 psi. This compared with an expected propellant ignition modulus of 990 psi, as documented in TR12874, ETM-3 Ignition Modulus for Fluid/Structural Interaction Analysis. Thus, no boot-strapping of the propellant grain will occur in ETM-3.

REFERENCES

[1] Wynn,R., "ETM-3 Ignition Modulus for Fluid/Structural Interaction Analysis," ATK Thiokol Propulsion, TR12874, Dec 2001.

[2] Ahmad, R. A., R. A. Morstadt, and A. M. Eaton, "RSRM and ETM03 Internal Flow Simulations and Comparisons," AIAA-2003-5104, AIAA/ASME/SAE/ASEE 39th Joint Propulsion Conference, Huntsville, AL, July 20-23, 2003

[3] Sorenson, K., "Final Test Report for ETP-1977, (ETM-3, TP-H1148 (Type VII) Propellant Standardization)," ATK Thiokol Propulsion, TWR-74361, April 2002

[4] Larsen, D., "TP-H1148 Birate Relaxation Modulus," ATK Thiokol Propulsion, TR13196, to be published.